

Supplementary Figure 1. Isolation of samples and replicates for RRBS analysis

a. Microdissection of polar body contaminants using laser ablation of the zona pellucida and aspiration with a piezo micromanipulator. Meiosis I and II polar bodies were mechanically removed in this fashion before collection of zygotic replicates (**Supplementary Movie 1**).

b. After microdissection, embryos were washed in Acid Tyrode's solution and through serial microdrops to eliminate remaining contaminants. Staining using the intercalating dye Hoechst 33342 confirmed an absence of genomic contaminants and revealed the two pronuclei.

c. To facilitate normal development, both 2-cell and later cleavage stages were biopsied after first cleavage using a similar strategy as that for zygotes.

d. Acid Tyrode mediated ablation of the zona pellucida and Hoechst staining revealed no detectable contaminants using our described isolation strategy in cleavage stage embryos.

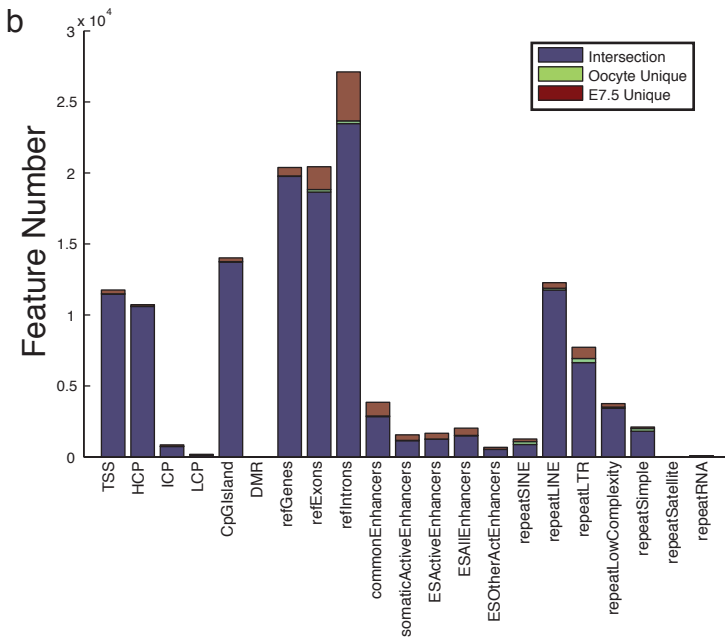
e. Zygote samples were isolated from natural matings using two visible pronuclei as a selective criteria. This restricted us to pre-syngamy embryos in which the pronuclei had not fused. Our scoring of each embryo was adopted from Ref 33 and representative examples are shown.

f. Pronuclear staging of triplicate replicates collected for RRBS analysis.

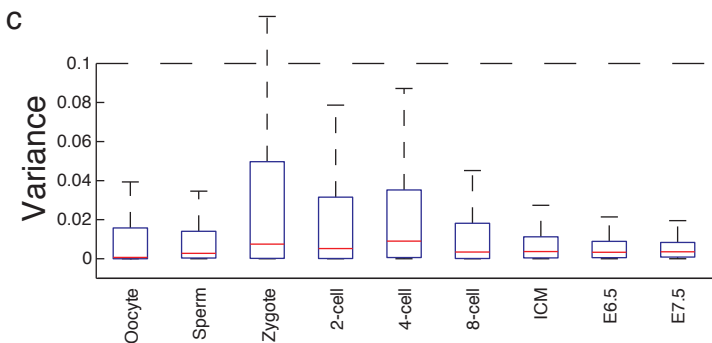
a

Sample	<i>n</i>	Input	Total CpGs (1x)	Total Unique (1x)	Mean Cov (1x)	Total CpGs (10x)	Total Unique (10x)	Mean Cov (10x)
Oocyte	4	~250 cells	54222070	1065085	53	53026780	754375	73
Sperm	5	~33 ng	49056060	1622074	30	46982560	1050991	44
Zygote	5	~63 cells	44368020	1657928	27	41760426	904473	45
2-cell	4	~100 cells	37411130	1624408	23	34903450	954615	36
4-cell	5	~170 cells	39351950	1706403	23	36791850	1029450	36
8-cell	3	~180 cells	41278790	1750977	24	38766400	1083324	36
ICM	5	~23 embryos	39284030	1535245	25	36594850	843261	36
E6.5	4	~6 embryos	59463460	1528915	39	58101030	1200623	48
E7.5	5	~6 embryos	62064200	1521215	41	61033030	1268909	48
Brain	2	50 ng	68372820	1627874	42	66613733	1120374	58
Heart	1	50 ng	57850729	1713221	34	55983685	1127397	50
Liver	2	50 ng	59559308	1545726	39	58036307	1126865	51

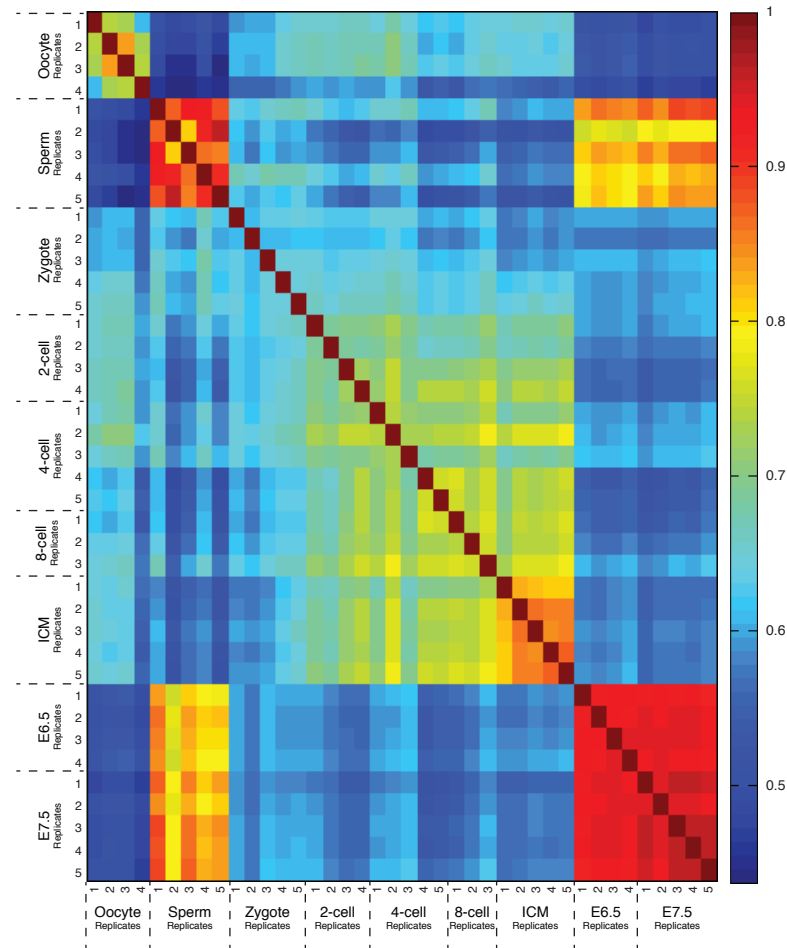
b



c



d



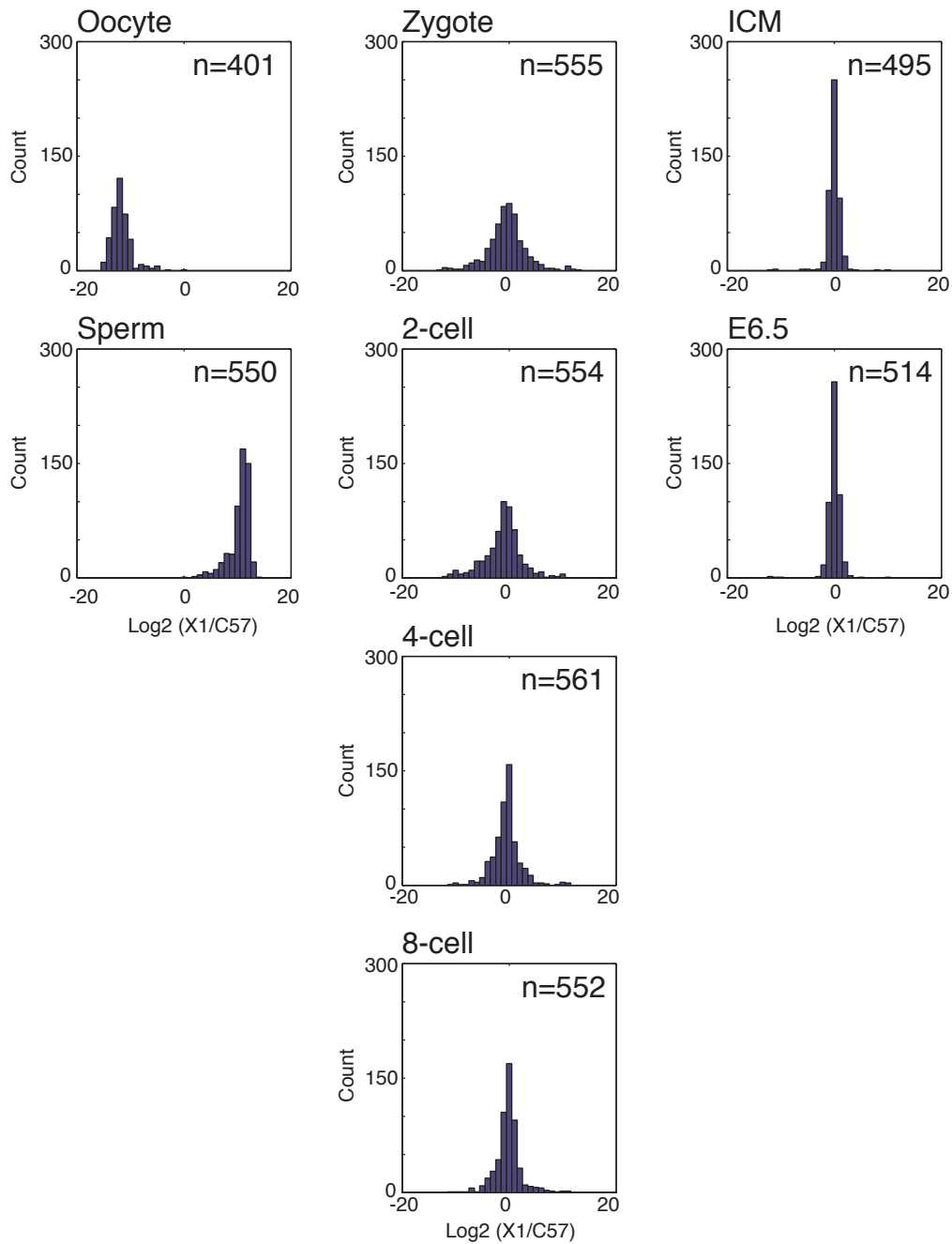
Supplementary Figure 2. Comparison of RRBS performance across stages and between replicates

a. Table of CpG coverage captured by RRBS including the number of replicates (*n*) at each stage, the average input per timepoint, the numbers of total and unique CpGs, and their mean coverage (Cov) at 1X or 10X.

b. The correspondence in the sampled features for different genomic annotations between single replicates of low input oocyte and higher input E7.5 embryo libraries. Blue: features covered by both samples; green: features covered in oocyte only; red: features covered in E7.5 only. Overall, there is mostly similar coverage of sampled features per library.

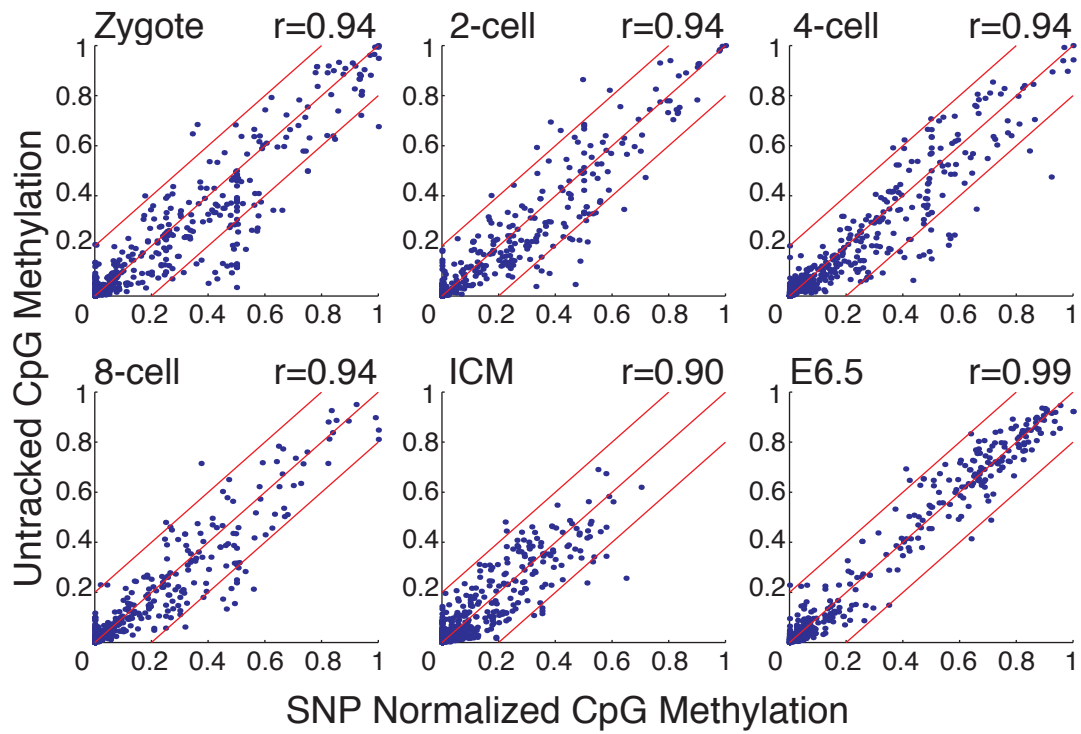
c. Boxplot of the variance across replicates at each stage. Red line indicates the median, edges the 25th/75th percentile and whiskers the 2.5th/97.5th percentile.

d. Pearson correlation coefficient heatmap between replicates and timepoints for all RRBS libraries used in these analyses. Correlation is generally higher within stages than between stages.



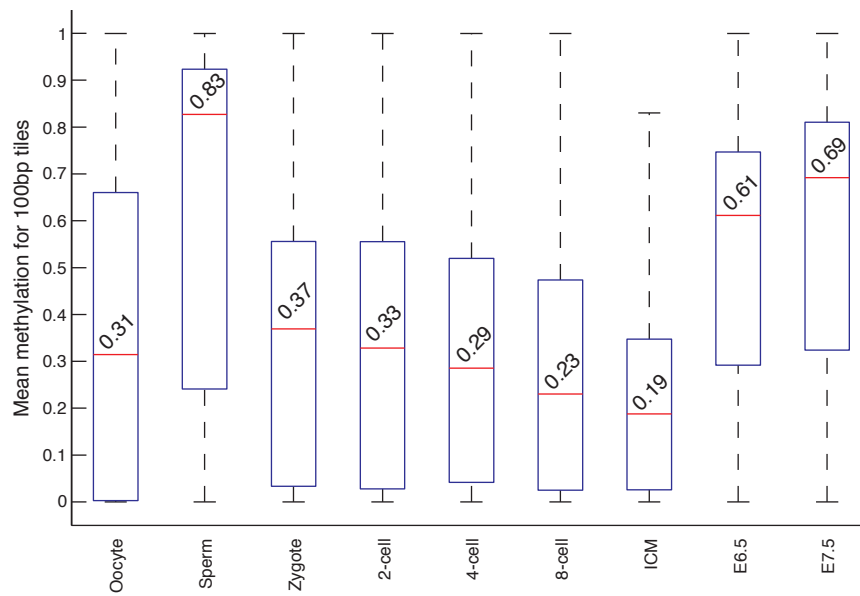
Supplementary Figure 3. Parent-of-origin Single Nucleotide Polymorphism (SNP) distributions for isolated gametes and hybrid embryos

Log odds ratio histograms for allelic frequencies for BDF1 (C57/B6 based) maternal and 129X1 paternal SNPs demonstrate minimal maternal biasing throughout the cleavage stages. The number of SNPs captured (n) for each time point is highlighted.

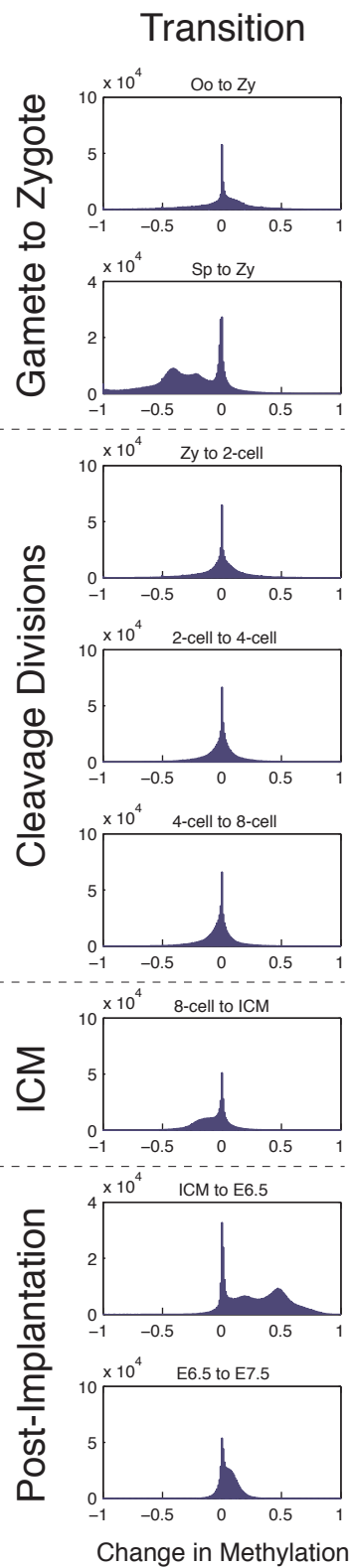


Supplementary Figure 4. Reported methylation values reflect their contributions from paternal and maternal alleles

Scatterplots depicting untracked methylation values against SNP normalized CpG methylation values for each stage in which hybrid crosses were used. Red lines indicate the $X=Y \pm 0.2$.



Supplementary Figure 5. Methylation values for 100bp tiles across pre-implantation development
 Boxplots of the methylation value per tile at each developmental stage. Red line indicates the median, edges the 25th/75th percentile and whiskers the 2.5th/97.5th percentile. The median value is shown above its line.



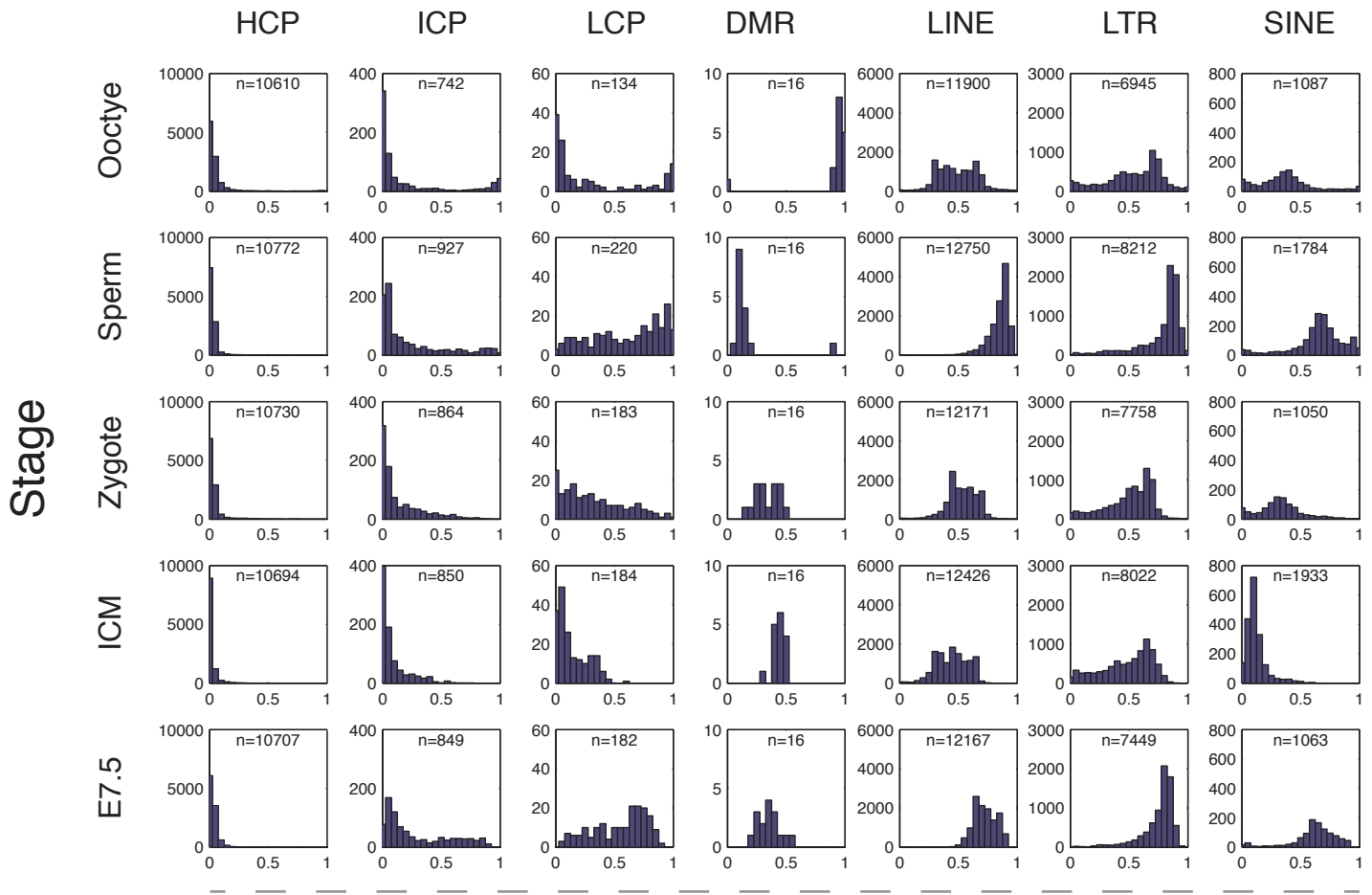
Supplementary Figure 6: Distribution of change in methylation levels in 100bp tiles between consecutive stages

Histograms show the distribution of the difference between all methylation values available for comparison between consecutive stages. There are two major transitions: (1) sperm to zygote and (2) ICM to E6.5. For other transitions, the difference is less skewed and reveals minimal change for these steps with gradual hypomethylation observed in the later cleavage stages and through ICM specification.

Feature Set

Promoter Classes

Repeat Classes

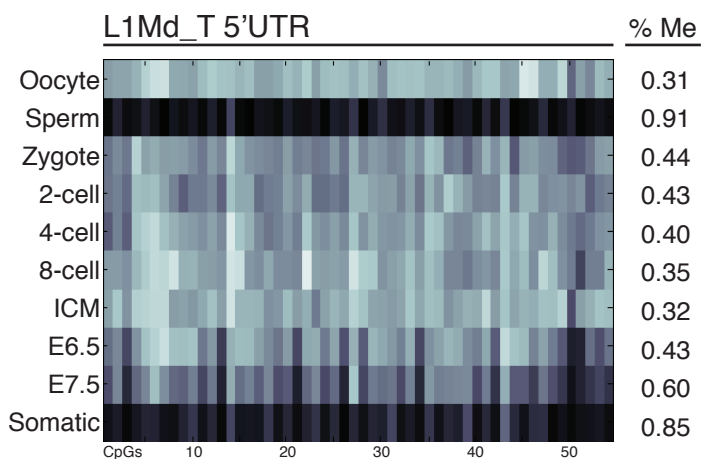


Feature Methylation

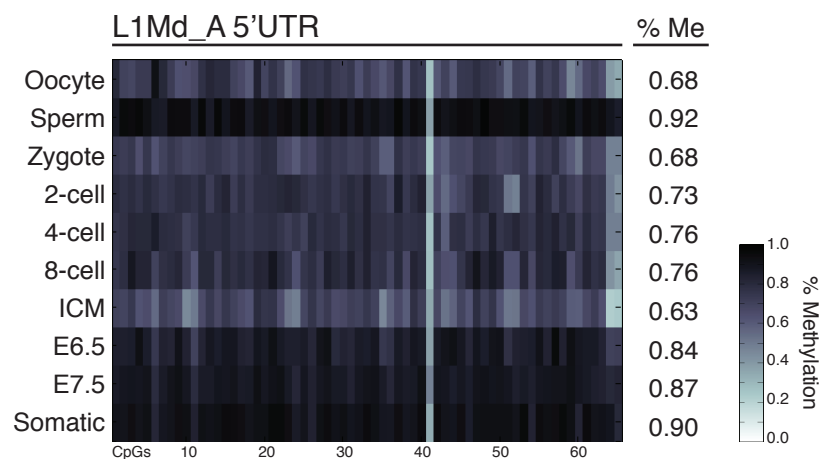
Supplementary Figure 7. Methylation histograms for genomic feature annotations throughout pre-implantation development

Notable dynamics at fertilization, across pre-implantation and upon specification of the embryo proper occur across multiple genomic feature sets. n indicates the number of genomic features captured at each time point.

a



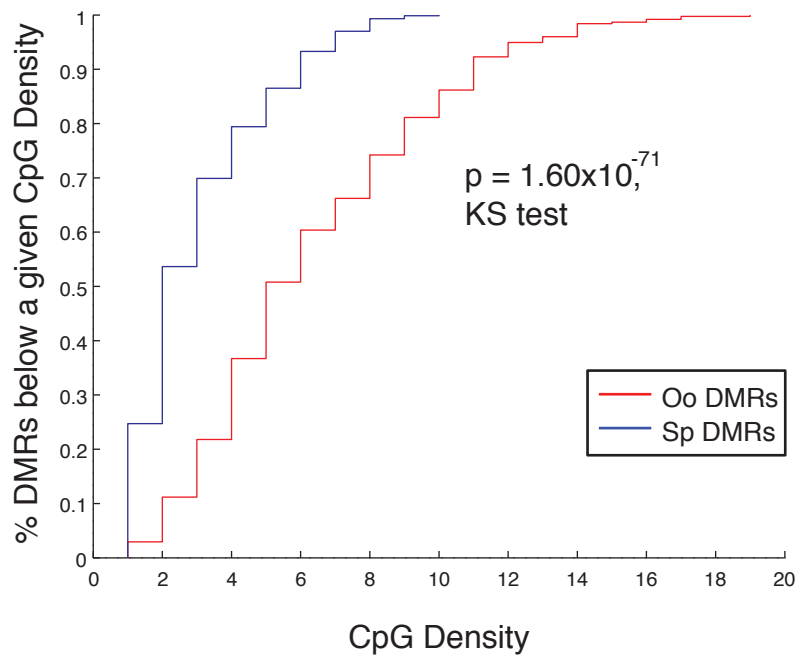
b



Supplementary Figure 8. Discrete methylation dynamics between different LINE-1 families

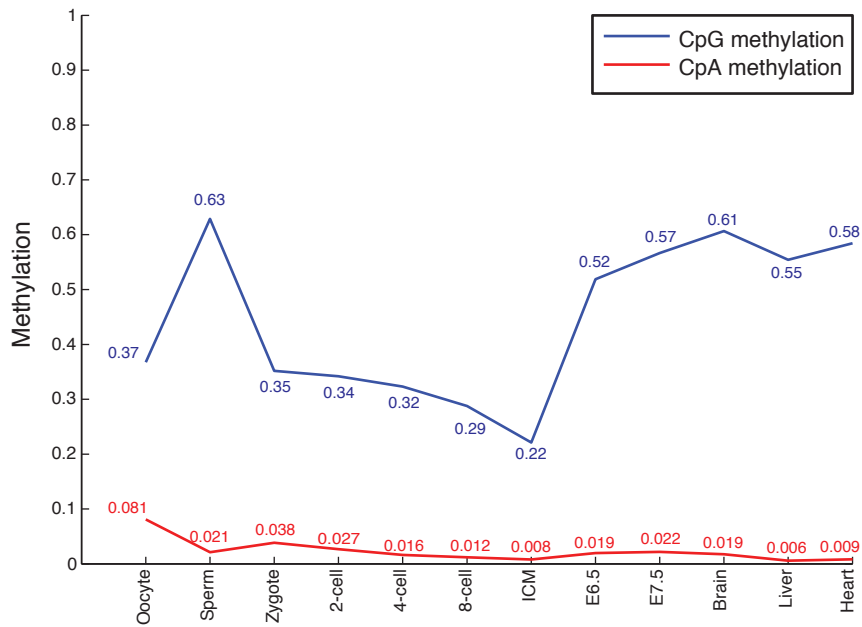
a. Heatmap for 54 individual CpGs covered within 1,495bp of a representative L1Md_T 5'UTR on Chr11 that dramatically loses methylation upon fertilization. Mean methylation levels for this element are highlighted on the right for each stage examined and recapitulate global observations for this feature.

b. Heatmap for 65 individual CpGs covered within 1,935bp of a representative L1Md_A 5'UTR on Chr11 that maintains comparatively higher and more uniform methylation throughout early embryonic development. Mean methylation levels for this element are highlighted on the right for each stage examined and recapitulate global observations for this feature as in **(a)**.



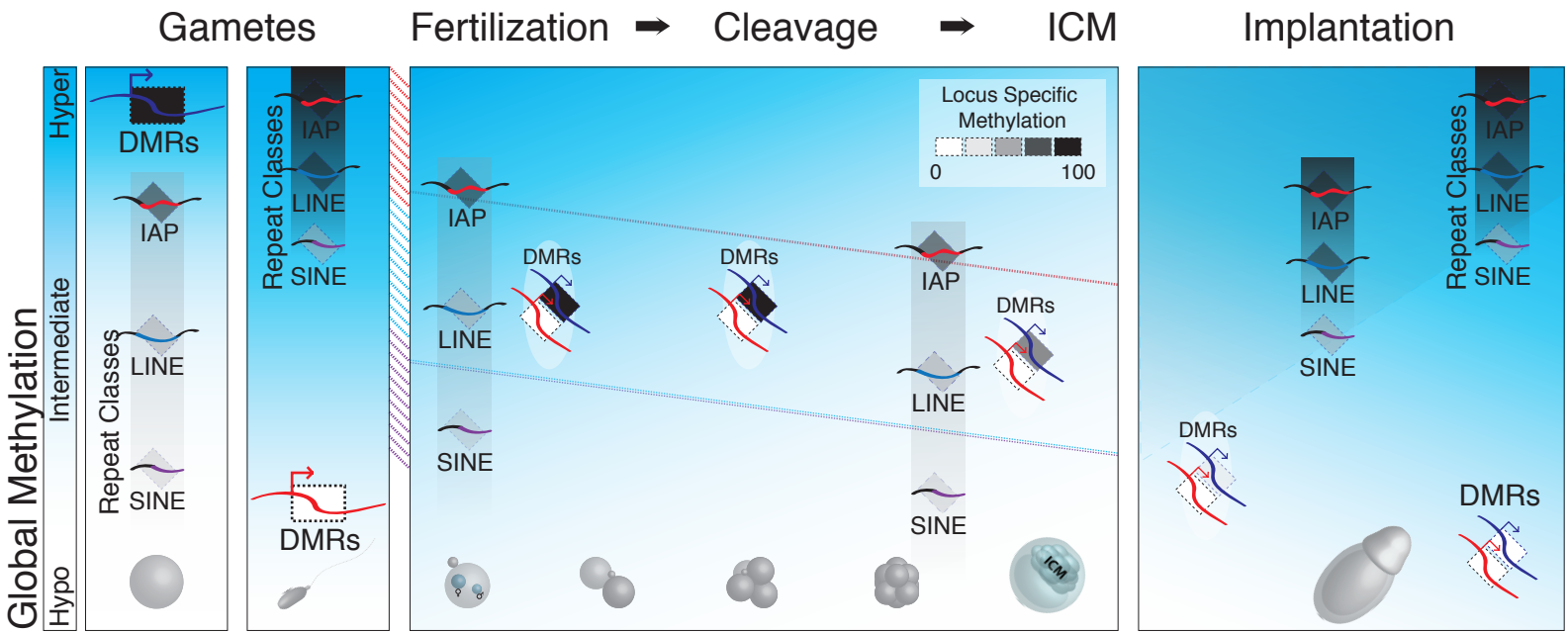
Supplementary Figure 9. Cumulative distribution function plot of CpG densities for oocyte- and sperm-contributed DMRs

The CDF (cumulative distribution function) plot displays the fraction of CpGs in the set that have a CpG density no greater than a certain value for oocyte- (red) and sperm- (blue) contributed DMRs. The median CpG density for each set is indicated by the X-axis value corresponding to $y=0.5$ (median CpG density is 6 and 2 for oocyte- and sperm- contributed DMRs, respectively). The CpG density dependence is significantly different between the two sets of DMRs ($P=1.6 \times 10^{-71}$; KS-test).



Supplementary Figure 10. Global CpG and CpA methylation dynamics during pre-implantation development

Mean CpG (blue) and CpA (red) methylation for 100bp tiles for each sample. Mean values are marked and reveal that CpA methylation is highest in oocyte and depletes throughout cleavage.



Supplementary Figure 11. A model for DNA methylation dynamics during early embryogenesis

Globally, each gamete exhibits unique methylation patterns genome-wide, with oocyte levels closely mirroring those of the pre-implantation embryo. Global methylation, as measured by bisulfite conversion, is moderately stable throughout cleavage, but diminishes to minimal values at the blastocyst/ICM stage. Specific repeat classes exhibit disparate methylation levels that are either retained as high (in the case of IAPs) or demethylated to lower values at the zygote stage (in the case of certain L1Md families and SINEs). Methylation values for these elements are maintained through cleavage stages before the somatic pattern is restored at gastrulation. Some CpG island promoters exhibit hypermethylation in the oocyte and these putative DMR signatures show retention of maternal CpG methylation through to the end of the cleavage stages before resolving to expected hypomethylation in the embryo proper.

Supplementary Table 1: Promoter methylation levels at fertilization and across early embryonic development

Methylation levels for Transcription Start Sites (TSS) covered by RRBS across early mouse development. Promoter density as defined in text is included, as are values for control adult somatic tissues.

Supplementary Table 2: Long Interspersed Element (LINE) retrotransposon feature methylation across early embryonic development

Respective coverage (in terms of elements covered) and mean methylation value for individual LINE families across early mammalian development and for control adult somatic tissues.

Supplementary Table 3: Long Terminal Repeat (LTR) retrotransposon feature methylation across early embryonic development

Respective coverage (in terms of elements covered) and mean methylation value for individual LTR families across early mammalian development and for control adult somatic tissues.

Supplementary Table 4: Designation and methylation status for identified oocyte-contributed Differentially Methylated Regions (DMRs)

Chromosome position, feature annotation, and methylation values across the pre-implantation timeline for 100bp tiles identified as oocyte-contributed DMRs. TSS name refers to the designated gene for DMR tiles that fall within a promoter.

Supplementary Movie 1: Polar body biopsy of a zygote sample collected for RRBS

Representative dissection of Meiosis I and II polar body contaminants from a fertilized zygote. The procedure starts with a short laser pulse that locally ablates the zona pellucida followed by aspiration of the Meiosis I, followed by the Meiosis II, polar bodies using a $8\mu\text{m}$ piezo pipette (see **Methods**).